




Increasing the Capping Efficiency of the Sindbis Virus nsP1 Protein Negatively Affects Viral Infection

Autumn T. LaPointe,^a Joaquín Moreno-Contreras,^b  Kevin J. Sokolowski^{a,c}

^aDepartment of Microbiology and Immunology, University of Louisville School of Medicine, Louisville, Kentucky, USA

^bDepartamento de Genética del Desarrollo y Fisiología Molecular, Instituto de Biotecnología, Universidad Nacional Autónoma de México, Cuernavaca, Morelos, Mexico

^cThe Center for Predictive Medicine for Biodefense and Emerging Infectious Diseases, University of Louisville School of Medicine, Louisville, Kentucky, USA

ABSTRACT Alphaviruses are arthropod-borne RNA viruses that are capable of causing severe disease and are a significant burden to public health. Alphaviral replication results in the production of both capped and noncapped viral genomic RNAs (ncgRNAs), which are packaged into virions during infections of vertebrate and invertebrate cells. However, the roles that the ncgRNAs play during alphaviral infection have yet to be exhaustively characterized. Here, the importance of the ncgRNAs to alphaviral infection was assessed by using mutations of the nsP1 protein of Sindbis virus (SINV), which altered the synthesis of the ncgRNAs during infection by modulating the protein's capping efficiency. Specifically, point mutations at residues Y286A and N376A decreased capping efficiency whereas a point mutation at D355A increased the capping efficiency of the SINV genomic RNA during genuine viral infection. Viral growth kinetics levels were significantly reduced for the D355A mutant relative to wild-type infection, whereas the Y286A and N376A mutants showed modest decreases in growth kinetics. Overall genomic translation and nonstructural protein accumulation were found to correlate with increases and decreases in capping efficiency. However, genomic, minus-strand, and subgenomic viral RNA synthesis were largely unaffected by the modulation of alphaviral capping activity. In addition, translation of the subgenomic alphaviral RNA (vRNA) was found not to be impacted by changes in capping efficiency. The mechanism by which the decreased presence of ncgRNAs reduced viral growth kinetics levels operated through the impaired production of viral particles. Collectively, these data illustrate the importance of ncgRNAs to viral infection and suggest that they play an integral role in the production of viral progeny.

IMPORTANCE Alphaviruses have been the cause of both localized outbreaks and large epidemics of severe disease. Currently, there are no strategies or vaccines which are either safe or effective for preventing alphaviral infection or treating alphaviral disease. This deficit of viable therapeutics highlights the need to better understand the mechanisms behind alphaviral infection in order to develop novel antiviral strategies for treatment of alphaviral disease. In particular, this report details a previously uncharacterized aspect of the alphaviral life cycle: the importance of noncapped genomic viral RNAs for alphaviral infection. This offers new insights into the mechanisms of alphaviral replication and the impact of the noncapped genomic RNAs on viral packaging.

KEYWORDS RNA processing, RNA virus, alphavirus, molecular biology

Alphaviruses are positive-sense, single-stranded RNA viruses which are capable of being transmitted between sylvatic vertebrate reservoir hosts and competent mosquito vectors in an enzootic cycle. During epizootic events, these viruses are

Received 23 October 2018 Accepted 8 November 2018 Published 11 December 2018

Citation LaPointe AT, Moreno-Contreras J, Sokolowski KJ. 2018. Increasing the capping efficiency of the Sindbis virus nsP1 protein negatively affects viral infection. *mBio* 9:e02342-18. <https://doi.org/10.1128/mBio.02342-18>.

Editor Jaisri R. Lingappa, University of Washington

Copyright © 2018 LaPointe et al. This is an open-access article distributed under the terms of the [Creative Commons Attribution 4.0 International license](https://creativecommons.org/licenses/by/4.0/).

Address correspondence to Kevin J. Sokolowski, kevin.sokolowski@louisville.edu.

capable of causing severe disease and are broadly categorized into two groups based on symptomology. Diseases caused by the encephalitic alphaviruses, such as Venezuelan equine encephalitis virus, are characterized by neurological symptoms and are capable of causing severe encephalitis, which may result in the death of the vertebrate host (1, 2). In contrast, the arthritogenic alphaviruses, such as Sindbis virus (SINV), Ross River virus (RRV), and chikungunya (CHIKV), cause disease ranging in severity from mild febrile illness to debilitating polyarthritis, which may persist for several months to years past the acute phase of infection (3–7). Despite the burden to public health posed by the alphaviruses, there are currently no effective and safe antiviral treatments for alphaviral disease.

During alphaviral infection, three viral RNA species are produced: the genomic strand, which encodes the nonstructural polyprotein, which is processed proteolytically to form the replication machinery; a minus-strand RNA template; and a subgenomic RNA, which encodes the structural proteins. The positive-sense alphaviral RNAs (vRNAs), namely, the genomic and subgenomic vRNAs, have a type 0 cap structure cotranscriptionally added to their 5' ends during RNA synthesis in order to protect the 5' end of the transcript and to facilitate translation after entry into the host cell (8–10). The addition of the 5' cap structure to the positive-sense vRNAs is a multistep process involving at least two alphaviral nonstructural proteins. Briefly, the methyltransferase domain of the alphaviral nsP1 protein catalyzes the addition of a methyl group from S-adenosylmethionine to a GTP molecule, forming a covalent m⁷GMP-nsP1 intermediate (11). Following the removal of the 5' γ -phosphate on the nascent vRNA molecule by nsP2, the m⁷GMP moiety is then transferred to the vRNA molecule by the guanylyltransferase activities of nsP1, resulting in the formation of the type 0 cap structure, 7^meGpppA (12, 13). Importantly, biochemical studies of alphaviral nsP1 proteins have found that both the methyltransferase activity and guanylyltransferase activity of nsP1 can be altered either negatively or positively via point mutations *in vitro* (14–16).

The presence of the type 0 cap structure on the alphaviral genomic and subgenomic vRNAs was first observed by paper electrophoresis, or thin-layer chromatography, of metabolically labeled vRNAs that were chemically and enzymatically degraded (8, 9, 17). Those studies further identified the sequences of the 5' termini of the alphaviral genomic and subgenomic vRNAs, which provided the first evidence for independent promoter initiation for the two positive-sense vRNA species (9). While those studies were able to identify the presence of the 5' type 0 cap structure, they were, by the nature of their design and technological limitations, unable to determine the relative frequencies with which the positive-sense vRNAs were capped.

Recently, we reported findings that indicated that the alphaviral genomic vRNAs are not ubiquitously capped and that a significant proportion of the genomic vRNAs produced during SINV and RRV infection lack the 5' type 0 cap structure (18). Furthermore, analyses of infectious and noninfectious viral particles demonstrated that both the capped and uncapped genomic vRNAs are packaged into viral particles throughout the course of infection. Through the use of tissue culture models of alphaviral infection, the presence of the uncapped vRNAs was found to correlate with the activation of a type I interferon (IFN) response. Moreover, an attenuated RRV mutant was found to produce fewer uncapped genomic RNAs than were produced by wild-type (WT) virulent RRV (18, 19). Collectively, these data were highly suggestive of an important biological role for the uncapped genomic vRNAs during infection; however, the precise functions of the uncapped genomic vRNAs during infection remained unknown.

The goal of this study was to determine the importance of uncapped vRNAs to SINV infection of tissue culture cells. Here, we show that the capping activity of SINV nsP1 is capable of being modulated, both positively and negatively, via the mutation of specific residues within the Iceberg region, a structurally organized region of cryptic function that is conserved among many viral capping enzymes (21). In addition, SINV infection was determined to be more detrimentally impacted by increasing the capping efficiency of SINV nsP1 than by decreasing the efficiency. Specifically, increasing the

rate of alphaviral capping negatively impacted viral growth kinetics by negatively affecting viral particle production. Collectively, our findings indicate that the non-capped vRNAs do play an important role during viral infection, and that decreasing the presence of noncapped vRNA impacts the viral life cycle at a fundamental level.

RESULTS

SINV vRNA capping can be modulated by point mutations in the nsP1 protein.

As described above, we recently reported that a significant number of the SINV genomic vRNAs produced during infection lack the type 0 5' cap structure. Despite being noninfectious, the noncapped viral genomic RNAs (ncgRNAs) are produced in a temporally dependent manner and are packaged into viral particles throughout the course of infection (18). Given the evolutionary conservation of the production of the ncgRNAs during alphaviral infection, we hypothesized that they must be biologically important to viral infection. This led us to question how modulating capping activity, which would alter the production of capped viral genomic RNAs and ncgRNAs, impacts viral infection. In order to determine the biological importance of the ncgRNAs during viral infection, we modulated the methyltransferase and guanylyltransferase activities of the alphaviral nsP1 protein to generate mutant SINV strains with either increased or decreased rates of viral capping. These mutations were based on previous work done in VEEV by Li et al. (14), where alanine substitutions at specific residues affected the nsP1 protein's methyltransferase and guanylyltransferase activities, as well as cap formation as a whole. Specifically, the previous study found that alanine substitutions at Y286 and N376 decreased RNA capping efficiencies, although to different extents, whereas an alanine substitution at D355 increased RNA cap formation. All three residues are highly conserved across multiple alphaviruses, including the model alphavirus SINV (Fig. 1A). Modeling of the SINV nsP1 protein using ITASSER indicated that residues D355 and N376 are likely close to one another, in parallel alpha helices proximal to the catalytic site within the Iceberg domain (Fig. 1B) (20). Nonetheless, Y286 is located at a distal site far from the putative active sites, as identified by prior mutational analyses (11, 12, 16). Admittedly, the ITASSER-predicted structure is unlikely to be a wholly accurate representation of the true structure of the SINV nsP1 protein. Despite the inherent inaccuracy of protein folding prediction algorithms in the absence of a closely related crystal structure, secondary and tertiary structural elements reminiscent of methyltransferase and guanylyltransferase enzymes may be detected, including a Rossmann fold-like structure surrounding the key residues involved in methyltransferase activity (16, 21). In addition, the overall arrangements of the core region and Iceberg regions are largely intact, and the known membrane anchoring domains face outward from the globular body of the protein (21). The differential abilities of Y286, D355, and N376 to affect VEEV nsP1 capping activity as well as their locations in highly conserved domains, which play integral roles in cap formation, made them strong candidates for testing how modulating the capping activity of nsP1 affects SINV infection.

In order to verify that the SINV nsP1 mutations altered the rate of vRNA capping, we assessed what proportion of viral particles contained capped RNA genomes. We have shown previously that both capped genomic RNAs and ncgRNAs are packaged and released during viral infection (18). Thus, knowing what proportion of capped viral RNA is being packaged into viral particles gives insight into the general capping efficiency of nsP1 during viral infection. To this end, the comparative assessment of viral capping efficiencies was accomplished by comparing the relative sensitivities of the mutants to RNase degradation using XRN-1, a 5'-3' exoribonuclease which preferentially degrades RNAs lacking a protective 5' cap structure, in particular, 5' monophosphate RNAs (22, 23). By measuring the amount of RNA resistant to XRN-1 degradation, we were able to determine what proportion of the total input RNA was capped relative to that seen with wild-type SINV, as the predominant noncapped 5' end was previously determined to be a 5' monophosphate (18). As shown in Fig. 1C, both SINV N376A and SINV Y286A had significantly lower proportions of XRN-1-resistant genomic RNAs than the WT strain,

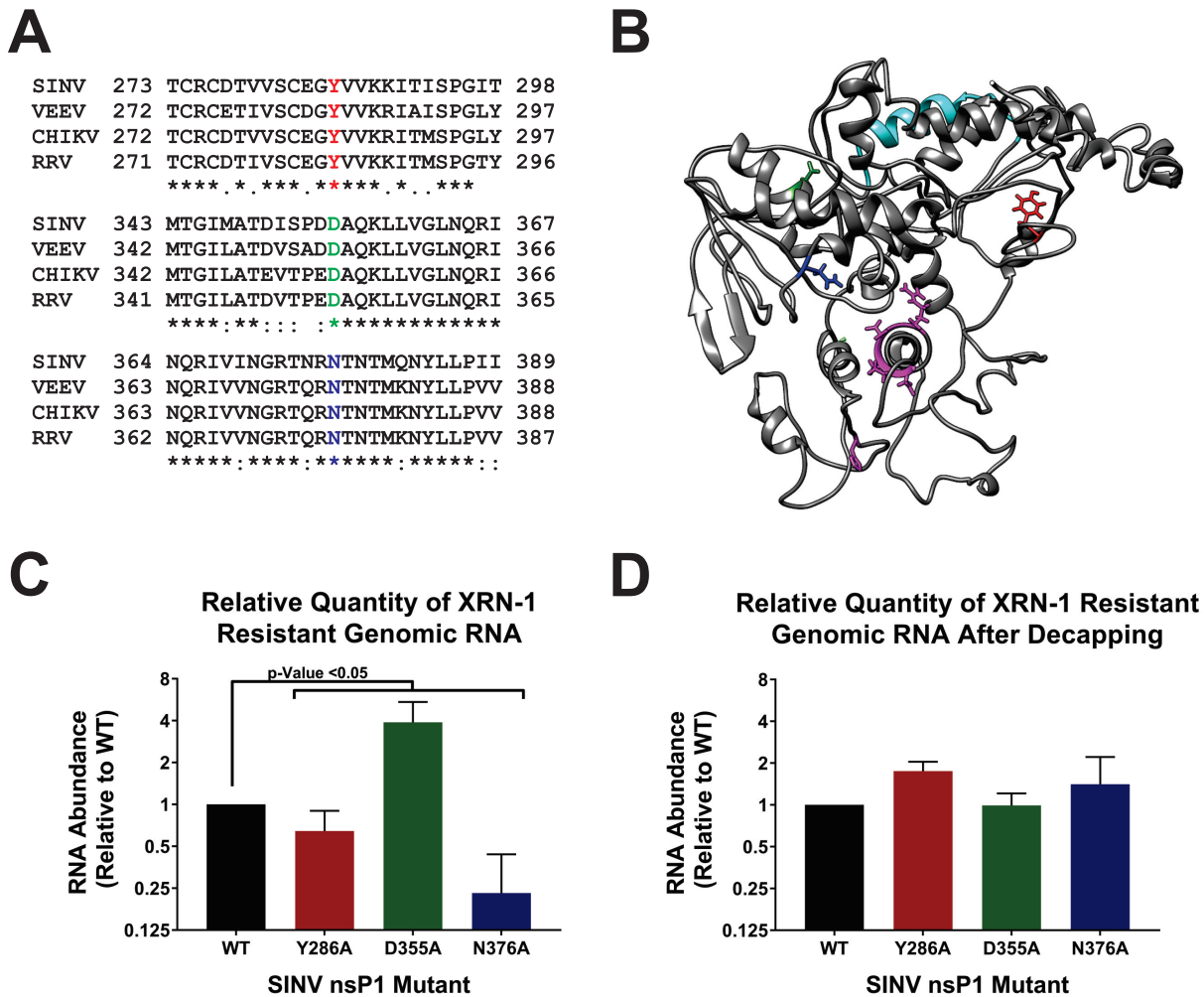


FIG 1 Point mutations in the nsP1 protein of SINV alter 5' vRNA capping efficiency. (A) Amino acid sequence alignment of selected alphavirus nsP1 proteins. The individual nsP1 protein sequences of Sindbis virus (ViPR accession no. [U38305](#)), Venezuelan equine encephalitis virus (VEEV; ViPR accession no. [L01443](#)), chikungunya virus (CHIKV; ViPR accession no. [DQ443544](#)), and Ross River virus (RRV; ViPR accession no. [GQ43359](#)) were aligned by the use of Clustal Omega. (B) An ITASSER-predicted structure of the SINV nsP1 protein. Amino acid residues of importance are highlighted as follows: red, Y286; green, D355; blue, N376; cyan, amphipathic helix; pink, residues involved in methyltransferase activities (including H39, which binds to the m^7 GMP residue). (C) Graph depicting the relative quantities of XRN-1-resistant vRNA isolated from viral particles produced by BHK-21 cells infected with wild-type SINV or the individual capping mutants at 24 hpi. (D) Identical to panel C, with the exception that the viral genomic RNAs were enzymatically decapped concurrently with XRN-1 treatment. All quantitative data shown represent means of data from a minimum of three independent biological replicates utilizing 3 independent particle preparations, with the error bars indicating standard deviations of the means. The *P* values indicated on the figure were determined by Student's *t* test.

with SINV Y286A having approximately 25% less XRN-1-resistant RNA than WT and SINV N376A having approximately 75% less XRN-1-resistant RNA. In contrast, and as expected from the previous study by Li et al. (14), SINV D355A was found to have a significantly greater proportion of XRN1-resistant RNA, with a mean approximately 4-fold greater than that observed for WT SINV. To confirm that the observed resistance of the SINV D355A genomic RNAs was due to a cap structure, the genomic RNAs were subjected to XRN-1 nuclease treatment in the presence of an established decapping enzyme (18, 24, 25). As shown in Fig. 1D, enzymatic removal of the 5' cap structure eliminated the resistance of the D355A-derived genomic RNAs to XRN-1 treatment, resulting in XRN-1 resistance levels comparable to those seen with WT SINV.

From these data, we were able to conclude that the point mutations engineered into the SINV nsP1 protein can indeed alter capping activity, both negatively, in the case of Y286A and N376A, and positively, as with D355A. Therefore, the individual nsP1 mutants can be used to assess the impact of the ncgRNAs by modulating the capping activity of nsP1 in tissue culture models of infection in a controlled manner.

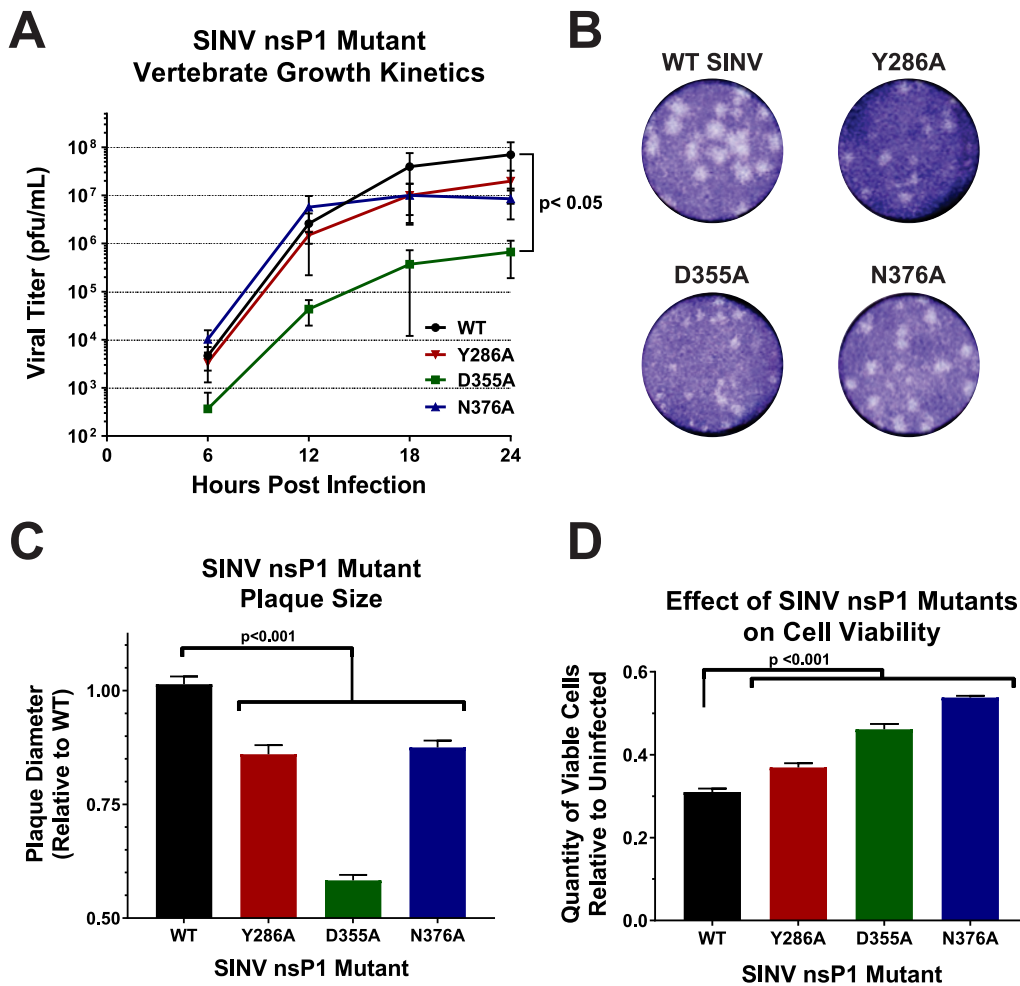


FIG 2 Altering viral capping efficiency negatively impacts viral infection. (A) Multi-step growth kinetics of the individual capping mutants and parental wild-type SINV as observed in BHK-21 cells infected at an MOI of 0.5 PFU/cell. Statistical significance was determined by analysis of the area under the curve. (B) Plaque morphology of wild-type SINV and capping mutant viruses in BHK-21 cells overlaid with 0.5% solution of Avicel at 24 h post-infection. (C) Graph indicating the average plaque diameter of the mutant viruses relative to wild-type SINV. Size was determined by ImageJ software (NIH). (D) Cell viability of BHK-21 cells infected with the individual capping mutants at 24 hpi relative to mock-infected BHK-21 cells. All quantitative data shown represent means of results from at least three independent biological replicates, with error bars representing standard deviations of the means. Statistical significance, as indicated within each panel, was determined by Student's *t* test.

Increased capping decreases SINV growth kinetics in mammalian cells. While the effects of synonymous point mutations on nsP1 capping efficiency have been previously characterized for VEEV at the enzymatic level (14), the effects of modulating capping activity on viral infection as a whole have not yet been studied in detail. Given the molecular function of the 5' cap structure, one could expect that the SINV nsP1 mutants that showed decreased vRNA capping would show impaired viral growth kinetics relative to wild-type virus. Likewise, if the ncgRNAs were truly nonfunctional, a mutant that increased capping would show enhanced viral growth kinetics with regard to wild-type infection. As demonstrated by the data presented in Fig. 2A, decreasing SINV capping modestly decreased viral growth kinetics levels, as observed for the SINV Y286A and SINV N376A mutants. However, the SINV D355A mutant, which showed increased vRNA capping relative to the WT, exhibited significantly decreased titers over the course of infection (Fig. 2A). In addition to a 2-log decrease in viral titer, the SINV D355A mutant produced plaques approximately half the size of those produced by wild-type SINV (Fig. 2B and C). Despite not showing significantly decreased viral growth kinetics, both the SINV Y286A and SINV N376A mutants also exhibited a small-plaque

phenotype, albeit not to the same extent as the SINV D355A mutant. In addition, all three capping mutants were found to have decreased induction of cell death compared to WT SINV (Fig. 2D).

Collectively, these data indicate that changing the efficiency of vRNA capping negatively impacted viral growth kinetics, illustrating that a step in the viral life cycle had been detrimentally affected. Furthermore, the viral growth kinetics data suggest that SINV is more sensitive to increased vRNA capping efficiency than it is to decreased capping efficiency. Thus, the ncgRNAs produced during infection are indeed biologically important. Nevertheless, despite the clear negative impact on viral infection, the precise nature of the molecular consequences of increased vRNA capping and decreased presence of ncgRNAs cannot be determined from these data alone. As such, the viral gene expression and vRNA synthesis profiles of each of the SINV nsP1 mutants were next assessed to determine if they were negatively affected by modulation of vRNA capping.

Translation of the SINV genomic RNA correlates with capping efficiency. For the majority of mRNAs, a key factor for determining whether or not an mRNA is translated is the presence or absence of a functional 5' cap structure (26–28). Therefore, changing the ncgRNAs to capped genomic RNAs or vice versa by altering viral capping efficiency should impact the amount of protein being produced by viral RNA during infection. To investigate the effect(s) that modulating nsP1 capping efficiency has on viral gene expression, a SINV reporter which contained the open reading frame of nanoluciferase in frame with the nsP3 nonstructural protein (18) was used to measure viral genomic RNA translation (Fig. 3A). Nanoluciferase expression was measured at regular intervals over the course of viral infection (Fig. 3B). As expected, the SINV D355A mutant, which showed increased capping relative to the wild type, exhibited increased genomic vRNA translation compared to WT SINV for every time point measured (Fig. 3C). Similarly, SINV N376A, which showed decreased capping relative to the wild type, showed decreased translation (Fig. 3C). Curiously, the SINV Y286A mutant showed differential nanoluciferase expression levels during infection, with translation levels being slightly increased very early during infection, decreased at 8 h post-infection (hpi), and similar to wild-type levels at later times post-infection.

While the use of the SINV nanoluciferase reporter virus allows the accurate quantification of viral gene expression during infection, it does not measure the sum accumulation of the nonstructural proteins. To measure the relative accumulations of the viral nonstructural proteins, the levels of SINV nsP2 protein were assessed via Western blotting at 8, 12, and 16 hpi. As shown in Fig. 4A and quantified in Fig. 4B, at 8 hpi, the accumulation of the SINV nsP2 proteins seen in SINV D355A and SINV N376A differed to a statistically significant extent from WT SINV. The abundance of nsP2 increased ~2.5-fold during SINV D355A infection relative to wild-type SINV infection. In contrast, nsP2 levels during SINV N376A infections were decreased ~2-fold relative to wild-type SINV infections. The levels seen with the SINV Y86A mutant were more or less equivalent to the wild-type nsP2 levels. Similar trends were observed at later times during infection. As depicted in Fig. 4C and D, the SINV D355A nsP2 levels at 12 hpi were statistically increased relative to those seen with the wild-type infection; however, given the low magnitude of the effect, these differences are unlikely to be biologically significant. In contrast, SINV D355A nsP2 levels at 16 hpi were increased to an extent that is likely biologically meaningful (Fig. 4E and F).

Overall, the levels of genomic translation for the SINV nsP1 mutants nicely reflect their differences in capping efficiency, with increased vRNA capping resulting in increased translation of the nonstructural proteins and decreased vRNA capping resulting in decreased translation at 8 hpi. These data are consistent with the conversion of the ncgRNAs to translationally competent capped genomic vRNAs. Furthermore, Western blotting confirmed the differences in translational activity detected during SINV nanoluciferase reporter infections. Taken together, the nanoluciferase and Western blot data indicate that the increased translation of the genomic vRNAs continues

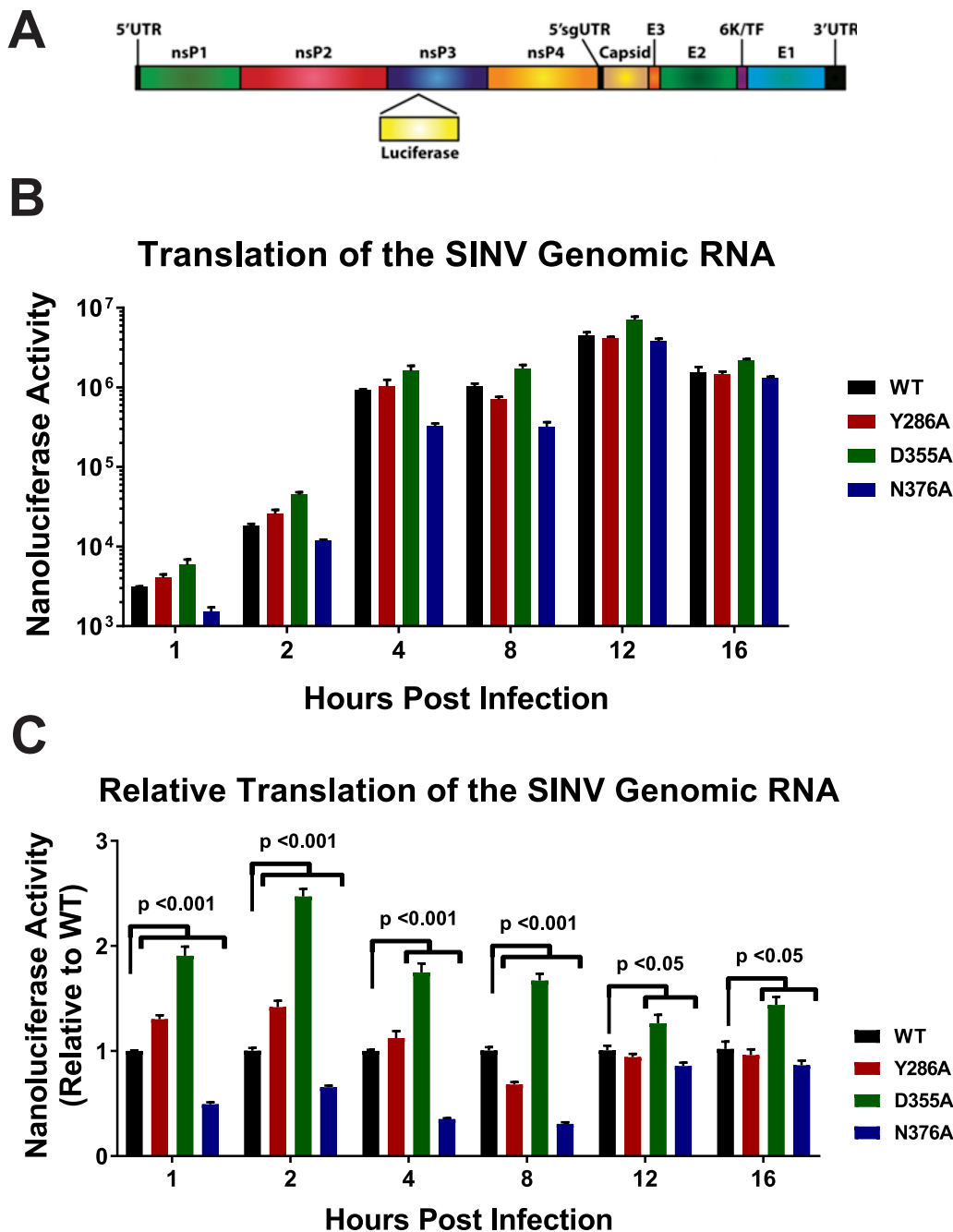


FIG 3 Translation of the genomic vRNA correlates with viral capping efficiency. (A) Schematic diagram of the SINV nanoluciferase reporter used in this study. UTR, untranslated region. (B) BHK-21 cells were infected with either the parental wild-type strain or an individual SINV capping mutant nanoluciferase reporter strain. The level of nanoluciferase activity was quantified at the indicated times post-infection. (C) The nanoluciferase activity, as reported in panel B, normalized to wild-type expression at each individual time point to enable readers to identify differences in translation. All the quantitative data shown represent means of results from three independent biological replicates, with the error bars representing standard deviations of the means. Statistical significances, as indicated in the figure, were first determined using analysis of variance (ANOVA) followed by *post hoc* statistical analyses by Student's *t* test.

during infection with SINV D355A beyond what is observed for wild-type SINV. Nonetheless, the biological differences in translational activity observed between the SINV D355A mutant and the corresponding parental wild-type strain fail to explain the approximately 200-fold reduction in viral titer.

Modulating SINV capping does not alter overall RNA synthesis or accumulation. Since differences in viral gene expression failed to explain outright the observed

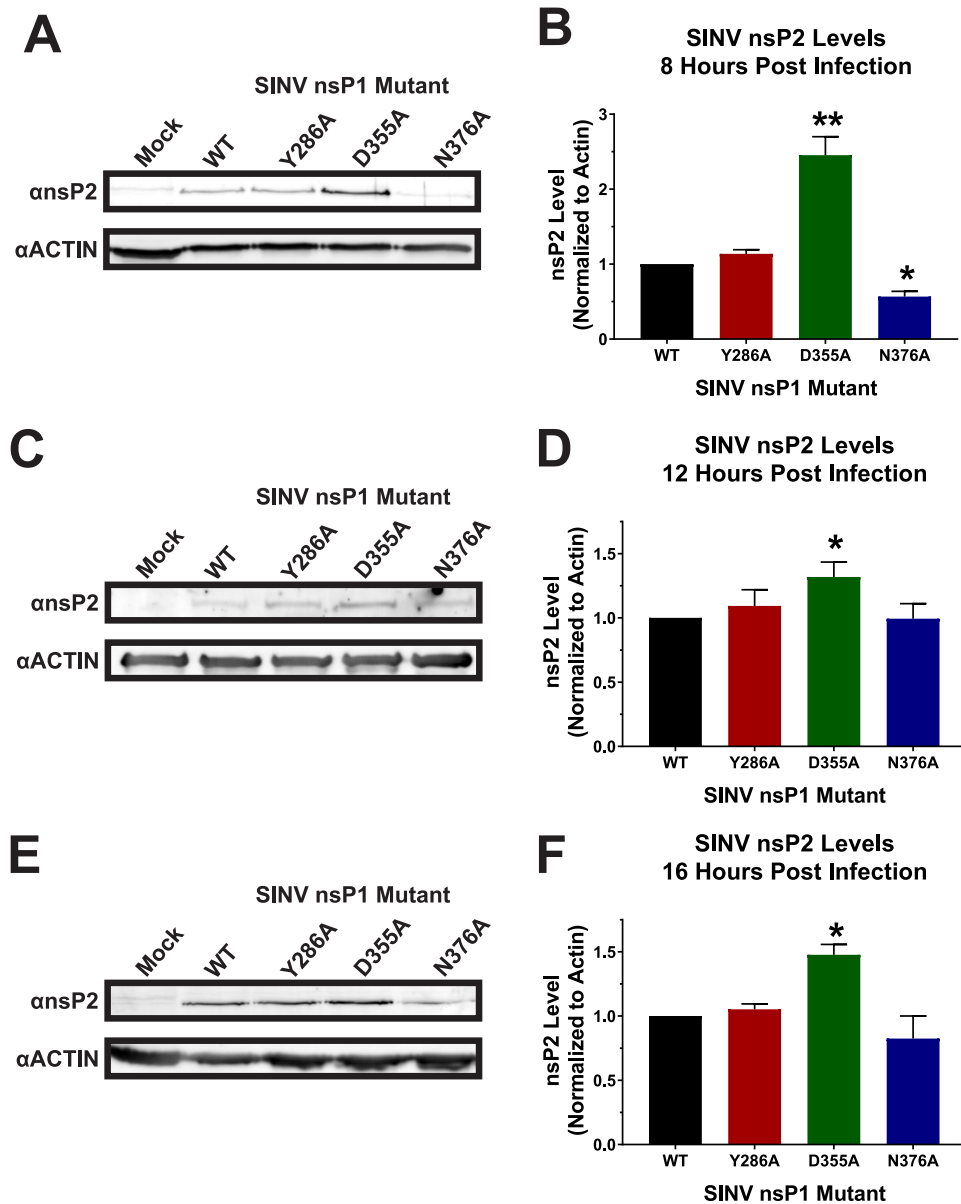


FIG 4 nsP2 protein levels are impacted by mutation of the nsP1 protein. (A) BHK-21 cells were infected with wild-type SINV or an individual capping mutant at an MOI of 5 PFU/cell and assessed by Western blotting to determine the abundance of nsP2 at 8 hpi. Actin is shown as a loading control. (B) Densitometric quantification of the nsP2 protein normalized to actin levels at 8 hpi. (C and D) Western blots and densitometry analyses identical to those described for panels A and B, respectively, with the exception that the timing of the assay coincided with 12 hpi. (E and F) Western blots and densitometry analyses identical to those described for panels A and B, respectively, with the exception that the timing of the assay coincided with 16 hpi. The Western blot images shown are representative of results of at least three independent biological replicates. All the quantitative data shown represent means of results from three independent biological replicates, with the error bars representing standard deviations of the means. Statistical significances, as indicated in the figure, were first determined using ANOVA followed by *post hoc* statistical analyses by Student's *t* test.

decreased viral titers associated with the SINV D355A mutant, we next sought to identify if vRNA synthesis was impaired as a result of nsP1 mutation. To determine what impact alteration of viral capping efficiency has on vRNA synthesis, the genomic, subgenomic, and minus-strand vRNAs were quantitatively assessed at 2, 4, and 8 h post-infection via quantitative reverse transcription-PCR (qRT-PCR). At 2 hpi, the SINV D355A mutant, which has increased vRNA capping relative to wild-type SINV, produced slightly more SINV genomic and subgenomic RNAs, whereas the SINV N376A mutant,

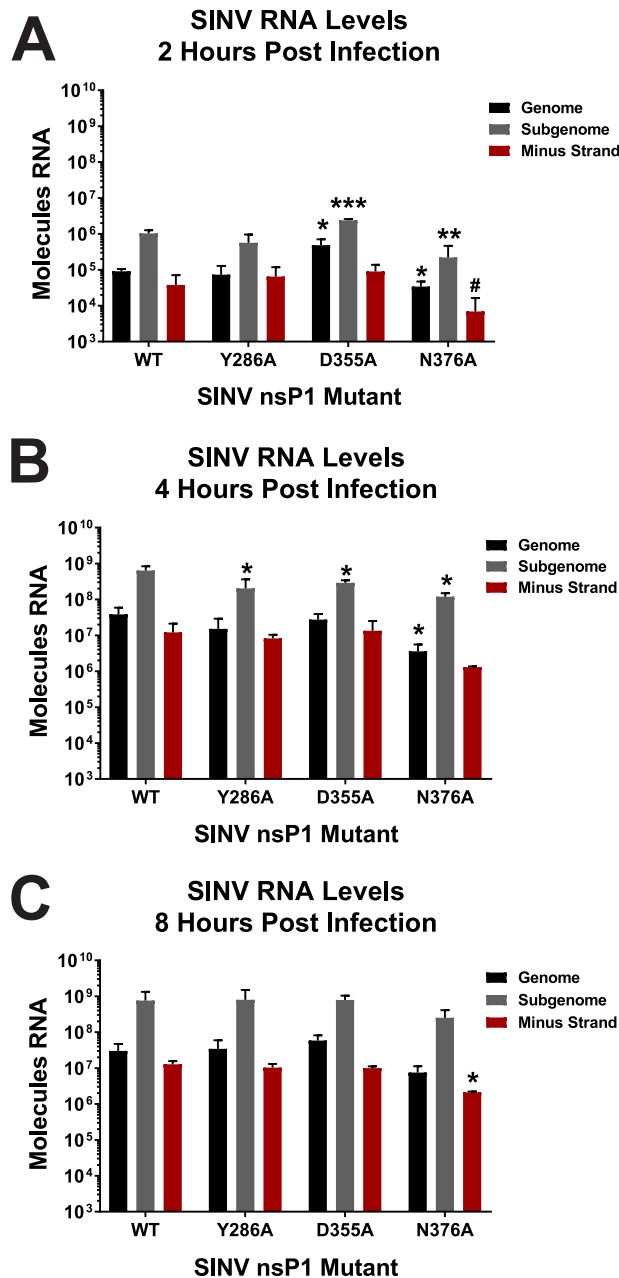


FIG 5 Altering vRNA capping efficiency impacts early RNA synthesis. (A) BHK-21 cells were infected with either wild-type parental SINV or an individual capping mutant virus at an MOI of 5 PFU/cell. At 2 h post-infection, the total cellular RNA was extracted and assessed for the absolute quantities of the genomic, subgenomic, and minus-strand vRNAs by qRT-PCR. (B and C) Identical to panel A, with the exception that the time points represent 4 and 8 h post-infection, respectively. All the quantitative data shown represent means of results from three independent biological replicates, with the error bars representing standard deviations of the means. Statistical significance data, as indicated in the figure, were first determined using ANOVA followed by *post hoc* statistical analyses by Student's *t* test. The *P* values determined by Student's *t* test are represented as follows: *, *P* < 0.05; **, *P* < 0.01; ***, *P* < 0.001. #, one of the biological replicates was below limit of detection, precluding meaningful statistical analysis.

which exhibits decreased vRNA capping, produced slightly fewer genomic and subgenomic RNAs compared to WT infection (Fig. 5A). In general, the differences in the amounts of genomic and subgenomic RNAs being produced by these two capping mutants are reflective of the differences observed in the synthesis of their replication machinery (Fig. 3 and 4). At 4 hpi, all three SINV nsP1 mutants showed a statistically significant deficit in the amount of subgenomic RNA present (Fig. 5B). Nonetheless,

these deficits are unlikely to be biologically meaningful due to their overall magnitude of effect relative to wild-type SINV. By 8 hpi, however, all three capping mutants showed levels of all three RNA species similar to the WT levels, with the exception of N376A, which had lower levels of minus-strand template than WT (Fig. 5C).

Altogether, these data demonstrate that altering the capping activity of nsP1 may have impacts on RNA synthesis very early during viral infection, but that these differences become muted as infection progresses. Importantly, these data indicate that vRNA synthesis on the whole had not been disrupted, precluding the possibility that the point mutations made in nsP1 had disrupted the function of the other nonstructural proteins. Moreover, similarly to that described above regarding viral gene expression in the previous section, the ~ 2 -log reduction in viral growth kinetics observed for the SINV D355A mutant was not due to decreased vRNA accumulation or defective vRNA synthesis.

Translation of the SINV subgenomic RNA is largely unaffected by viral capping.

Given that neither the differences in nonstructural gene expression nor the differences in vRNA synthesis were sufficient to explain the negative impact of the SINV nsP1 D355A mutation, we next sought to determine whether the function of the subgenomic vRNAs had been impacted. As both the genomic and subgenomic vRNAs are capped by nsP1, it was hypothesized that mutations which increased capping of the genomic vRNAs might impact subgenomic vRNA function. As such, it could be expected that these vRNAs would exhibit responses similar to those seen with altered capping in terms of translation. In order to determine whether translation of the subgenomic vRNAs had been impacted similarly to results seen with the genomic vRNAs, the amount of protein produced late during infection was measured using metabolic labeling (Fig. 6A). Curiously, both the SINV D355A and SINV N376A mutants exhibited a modest decrease in viral capsid production (Fig. 6B). In addition, none of the SINV nsP1 mutants exhibited differences with regard to the shutoff of host translation (a hallmark of alphaviral infection, as reviewed in reference 29), as evidenced by the labeling of the cellular actin protein, relative to WT SINV (Fig. 6C). Interestingly, however, ongoing synthesis of a high-molecular-weight protein consistent with the characteristics of the nonstructural polyprotein was reproducibly detected during the metabolic labeling of SINV D355A mutant infections.

Collectively, these data indicate either that changes in the capping efficiency of the genome might not lead to equivalent changes in capping of the subgenomic vRNA, or alternatively, that SINV, and likely other alphaviruses, regulates the translation of the structural proteins differently from the nonstructural proteins (30). Regardless, these data suggest that subgenomic translation and host translational shutoff are not impacted to a biologically significant degree by modulating the efficiency of vRNA capping and thus are not responsible for the decreased viral titer associated with increased capping efficiency.

Increasing SINV capping decreases viral particle production. Given that the molecular characterizations of the SINV nsP1 mutants had so far failed to identify the molecular defect leading to decreased viral growth kinetics of the SINV D355A mutant, we expanded our analyses beyond the life cycle events most obviously affected by the 5' cap structure. Since vRNA synthesis and viral gene expression were unaffected, we next sought to determine whether viral particle assembly was negatively impacted by increases in the capping efficiency of the SINV nsP1 protein.

To determine whether increases in capping efficiency affected viral particle production, we quantified the total number of particles produced by each mutant as well as by wild-type SINV after 24 h of infection. Similarly to what was observed during the kinetic analyses of viral infection, increased vRNA capping was associated with the production of significantly fewer particles, with the SINV D355A mutant producing ~ 25 -fold-fewer particles (as measured by genome equivalents per milliliter) than wild-type SINV (Fig. 7A). In contrast, particle production was largely unaffected during infections of the SINV Y286A and SINV N376A mutants, which decreased vRNA capping.

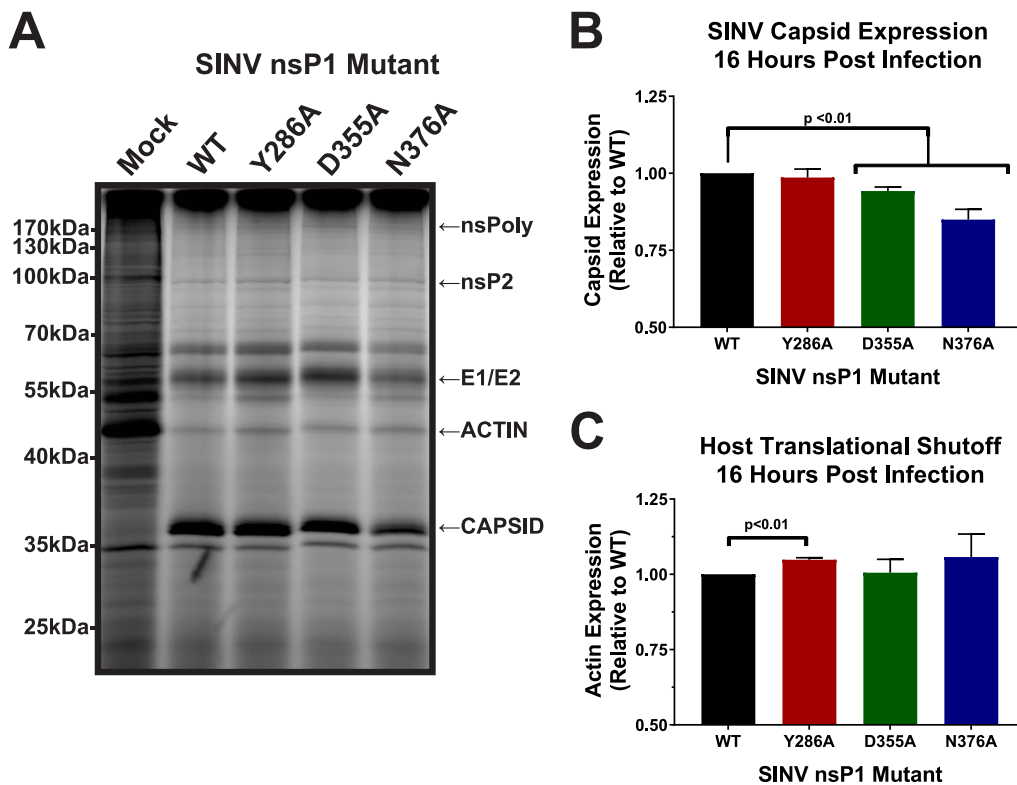


FIG 6 Subgenomic gene expression is unaffected by altering SINV vRNA capping. (A) BHK-21 cells were either mock treated or infected with wild-type SINV or an individual capping mutant at an MOI of 10 PFU/cell. At 14 hpi, the cells were pulsed with L-AHA for a period of 2 h. The cells were then harvested, and equal cell volumes of cell lysate were analyzed by SDS-PAGE and fluorescent imaging. The data shown are representative of results from three independent biological replicates. (B) Densitometric quantification of the SINV capsid protein, with intensity relative to wild-type SINV shown. (C) Densitometric quantification of the host actin protein, with intensity relative to wild-type SINV shown. All the quantitative data shown represent means of results from three independent biological replicates, with the error bars representing standard deviations of the means. Statistical significance was determined by Student's *t* test.

The point mutations utilized in this study are located within, or closely adjacent to, the SINV packaging signal (31). Previous characterizations of the alphaviral packaging signals have indicated the importance of stem-loop structures which contained a guanosine triplet in the loop region. Mutational analyses of the alphaviral packaging elements determined that mutation of the guanosine triplets, or deletion of the packaging element altogether, significantly reduced viral titer due to nonselective particle assembly leading to the production of alphaviral particles containing the subgenomic vRNAs (31). Further experiments revealed that a minimum of two guanosine triplet stem loops was sufficient to impart wild-type particle production with selectivity for the genomic RNA. Even though none of the point mutations used in this study impact either the guanosine triplets or the general secondary structures (as predicted by *in silico* analysis), the potential for the inhibition of assembly by a noncapping mechanism existed, warranting further assessment of particle production during SINV nsP1 mutant infections. As mentioned earlier, disruption of the alphaviral packaging signal leads to the production of viral particles containing predominantly subgenomic RNAs (31). As shown in Fig. 7B, quantitative determinations performed to identify which specific vRNAs were packaged into wild-type and SINV nsP1 mutant viral particles indicated no aberrant packaging of the SINV subgenomic RNA, consistent with an intact functional packaging signal.

The high degree of similarity between the relative magnitude of effect regarding decreased viral titer and viral particle production during SINV D355A infection indicates that particle assembly, and not the slight perturbations in vRNA synthesis or structural gene expression, is primarily responsible for decreased viral growth kinetics. Impor-

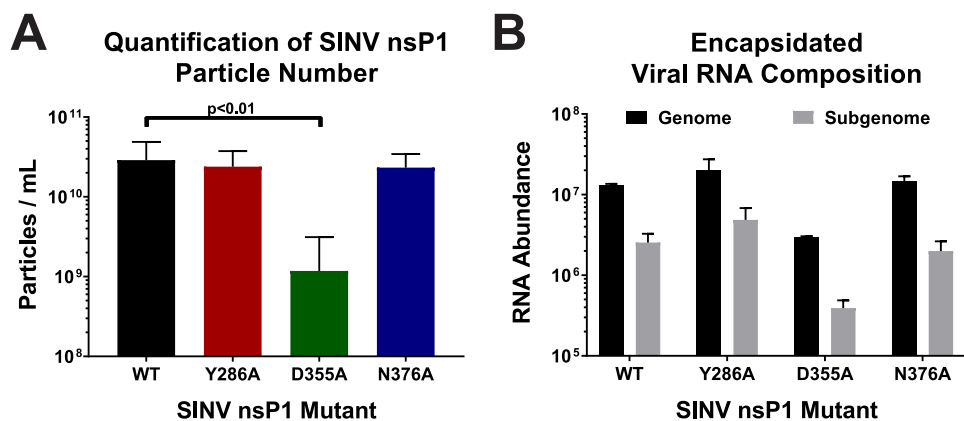


FIG 7 Analysis of SINV particle production. (A) BHK-21 cells were infected with either wild-type SINV or an individual capping mutant at an MOI of 5 PFU/cell. At 24 hpi, the total number of viral particles produced was measured using qRT-PCR. Data shown represent means of results from at least 6 independent biological samples. (B) Quantitative determination of the composition of the encapsitated viral RNAs in mature extracellular viral particles. Samples of virus-containing supernatants were assessed to determine the absolute quantities of the genomic and subgenomic RNAs via standard curve qRT-PCR. All the quantitative data shown represent means of results from three independent biological replicates, with the error bars representing standard deviations of the means. Statistical significance data, as indicated in the figure, were first determined using ANOVA followed by *post hoc* statistical analyses by Student's *t* test.

tantly, these data suggest that SINV, on the whole, was much more tolerant of mutations which decreased capping efficiency than of those that increased capping efficiency and that, by increasing the capped-to-noncapped viral RNA ratio, viral particle production had been detrimentally affected. Moreover, these data validate the idea that the packaging signal remains functional in the presence of the nsP1 point mutations described in this study.

DISCUSSION

The capping of SINV genomic vRNAs can be modulated by point mutations in nsP1. The data shown in Fig. 1 indicate that, in SINV, 5' capping of the genomic vRNA can be modulated via single-point mutations in the nsP1 protein. This is true for both increases in vRNA capping, as seen with SINV D355A, and decreases in capping, as seen with SINV Y286A and SINV N376A. Moreover, vRNA capping can also be modulated to different extents, as seen with SINV Y286A and SINV N376A, which decreased vRNA capping by 25% and 75%, respectively. The ability to change nsP1 capping efficiency in a controllable manner opened up new avenues to explore the molecular and biological importance of both the capped genomic vRNAs and the ncgRNAs during infection in tissue culture models of infection and *in vivo*.

From the data above, we may conclude that a primary consequence of mutating the SINV nsP1 protein is the alteration of vRNA capping. Nonetheless, the alphaviral nonstructural proteins interact with one another during infection (32–35). Previous studies have shown that disrupting these interactions by mutation results in poorer viral infection and, more specifically, leads to severe defects in vRNA synthesis (32–34). However, the disruption of nonstructural protein interactions is unlikely with the nsP1 mutants reported in this study, as the phenotypes described for situations where the interactions between the nonstructural proteins have been disrupted are inconsistent with what is reported here. For example, several residues in nsP4 have been reported as important for interactions with nsP1, such as G38L in nsP4 (32). When that residue was mutated in nsP4, viral infection exhibited decreased growth kinetics and a small-plaque phenotype. However, a hallmark of disruption of the nonstructural protein interactions was the severely decreased synthesis of minus-strand vRNA throughout the course of infection (32, 34). As shown in Fig. 5, none of the nsP1 mutants examined in this study exhibited a significant deficit in production of any viral RNA species, with the exception of a minor decrease in minus-strand vRNA synthesis by N376A. It is of

note that the nsP4 G38L mutant was able to be rescued by an additional mutation in nsP1 at N374 (32). The nsP1 N374 mutation resulted in complete restoration of viral titer and partial restoration of minus-strand vRNA synthesis in the nsP4 G38L background compared to the wild type. While the effect of mutating nsP1 N374 on capping efficiency is not known, one could speculate that, given its proximity to other residues which we have shown to alter capping activity, modulating the capping efficiency of nsP1 could be a way of coping with the detrimental nsP4 G38L mutation, which creates a severe defect in RNA synthesis. In addition to this, a previous report noted that the region in nsP1 encompassing the SINV point mutations utilized here exhibits little to no interaction with the nsP2 protein (35). Thus, for the reasons described above, the nsP1 residues mutated during this study are likely not involved in mediating nonstructural protein interactions, and the resulting deficits in the viral life cycle are not due to disrupted nonstructural protein interactions.

SINV infection is more sensitive to increased capping than to decreased capping. Multiple studies have shown that polymorphisms in nsP1 have profound effects on virulence. Mutations in regions of nsP1 have been shown to alter vRNA synthesis, viral titer, viral sensitivity to IFN, and disease severity *in vivo* (19, 32, 36). Certain residues, such as nsP1 H39 in SINV, completely abrogate viral infection when mutated by eliminating the methyltransferase activity of the nsP1 protein (15, 16, 37). Therefore, we expected that incorporating the point mutations which alter viral capping would have an impact on viral infection. However, we were surprised to find that while the mutant associated with increased capping was found to have decreased viral growth kinetics, the results seen with the mutants associated with decreased capping were not significantly different from those seen with wild-type SINV (Fig. 2A). This result was especially surprising given that it was found that all three capping mutants had small-plaque phenotypes and decreased cell death, yet D355A was the only mutant to show altered growth kinetics (Fig. 2B, C, and D). Serial passaging of the mutants used in this study indicated that they were stable for at least 4 subpassages, as no reversion events (based on plaque phenotype) were observed for any of the SINV nsP1 mutants. This suggests that SINV is more detrimentally impacted by changes which increase the amount of capped vRNA present than by those which decrease capping efficiency. Thus, increases in the capping efficiency of the SINV nsP1 protein, which effectively reduced the production of the ncgRNAs, indicate that the ncgRNAs are biologically important to viral infection.

Altering capping leads to changes in genomic translation but not RNA synthesis or subgenomic translation. As would be expected, changes in nsP1 capping efficiency correlated with changes in genomic vRNA translation. In addition, the reduced presence of the ncgRNAs correlated with increased translation of the viral genomic RNA throughout infection, as can be seen with the SINV D355A increased-capping mutant. Furthermore, decreasing the capping efficiency of the nsP1 protein, as evidenced by the SINV N376A mutant, modestly decreased translation. Admittedly, the second decreased-capping mutant, SINV Y286A, did not follow the same pattern as the SINV N376A mutant. This may have been due to the comparatively minor decrease in capping efficiency caused by SINV Y286A not having been significant enough to consistently alter the vRNA population, leading to dysregulated genomic translation.

However, the increased translation exhibited by the SINV D355A mutant did not lead to lasting compounding biological effects, at least in tissue culture models of infection. For instance, despite more replication machinery having been produced early during SINV D355A infection, there were no overt differences in the levels of synthesis of any of the viral RNA species at the time points tested (Fig. 5). This suggests that increasing or decreasing the production of the nonstructural proteins alone is not enough to alter RNA synthesis over the long term in highly permissive tissue culture models of infection. Nonetheless, due to technical limitations we were unable to accurately assess vRNA synthesis earlier than 2 h post-infection. Hence, the possibility that vRNA synthesis is enhanced very early during infection remains unaddressed.

Another unexpected result was that changes in capping efficiency seemed to affect subgenomic translation differently than genomic translation. The data presented in Fig. 6 show that both the increased-capping and decreased-capping mutants SINV D355A and SINV N376A demonstrated slight, biologically nonsignificant decreases in capsid production at 16 hpi, despite showing notable differences in nonstructural gene expression (Fig. 3 and 4). This suggests either that capping efficiency is regulated differently for the subgenomic RNA than for the genomic RNA, resulting in no differences in capping efficiency for the subgenomic RNA, or that translation of the subgenomic RNA is less dependent on the presence of a 5' cap than that of the genomic RNA during infection. The latter speculation is supported by previous studies which demonstrated that the eukaryotic initiation factor 4F (eIF4F) complex, which includes cap-binding eIF4E, is not needed to initiate translation of the alphaviral subgenomic RNA (30, 38). Those previous studies, along with the data presented here, suggest that translation of the subgenomic RNA is unaffected, at least in part, by modulation of vRNA capping.

In addition to there being little effect on subgenomic translation, there were also shown to be no differences in terms of host translational shutoff between any of the capping mutants and WT SINV (Fig. 6C). This further supports the idea that the point mutations made in nsP1 were not negatively affecting interactions between nonstructural proteins, because disruptions between nsP1 and nsP4 have been previously found to negatively affect host translational shutoff (32). Host translational shutoff, at least for SINV, has been largely attributed to the translation of the structural proteins (39). Therefore, it is unsurprising that there is no difference in host shutoff between the capping mutants and the WT SINV given that there is little difference in subgenomic expression.

Decreased titer due to changes in capping caused by interference with particle production. The decreased viral growth kinetics observed during SINV D355A infection correlated remarkably with decreased particle production. However, the congruence of the decreases in the levels of infectious units and viral particles indicates that the levels of viral infectivity are more or less identical for all of the viral strains. The discrepancy between the two magnitudes of effect (an approximate 5-fold difference) is likely due to confounding variations in the accuracy and precision of the two measurements. Nonetheless, it remains possible that the viral particles have differences in their basal infectivity characteristics. Studies examining earlier effects of the ncgRNAs are ongoing and will be presented in a follow-up study.

The observation that decreased particle production was the primary molecular defect during SINV D355A infections suggests that increasing the amount of capped genomic RNAs, thereby decreasing the number of ncgRNAs, negatively impacts the assembly of nascent viral particles. Whether the increased capping activity is directly or indirectly responsible for the packaging phenotype is not definitively known. Characterizations of SINV packaging have indicated that selectivity remains intact during the SINV D355A assembly process despite decreased particle production overall, as packaging of subgenomic vRNAs was not observed. This is indicative of a functional alphaviral packaging signal despite the incorporation of minor point mutations into the region defined as the packaging signal for SINV. Moreover, the SINV Y286A mutation which also resides within the SINV packaging element lacks an appreciable packaging phenotype. Thus, the assembly phenomena associated with the SINV D355A mutant cannot be simply explained by disruption of the alphaviral packaging signal.

While the underlying mechanism is unclear, the data presented above indicated that nonstructural protein expression is increased relative to the level seen with the wild-type parental virus and remains increased well into the late stages of infection during SINV D355A infections. Collectively, these data indicate that decreasing the production of the ncgRNAs perturbs viral genomic RNA function beyond the individual RNA level, as apparent compounding effects on the genomic RNA population are observed. Precisely how the translationally inactive ncgRNAs serve to modulate genomic vRNA function as a whole, leading to efficient particle assembly, is unknown.

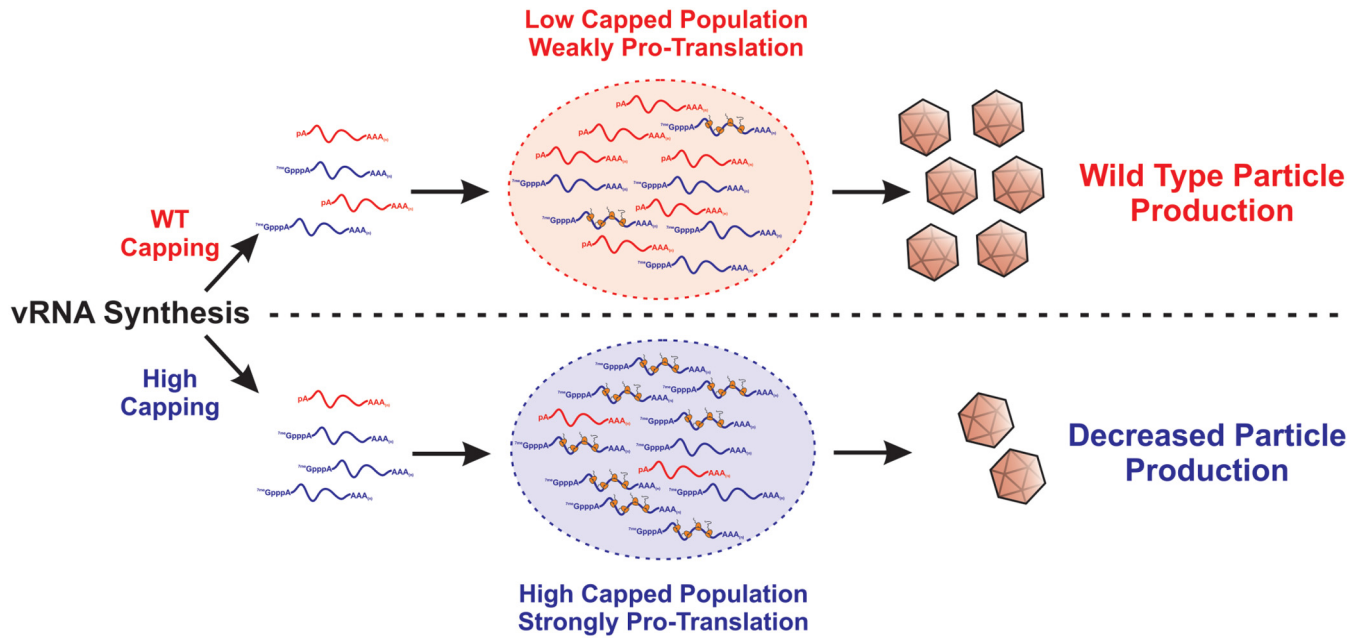


FIG 8 Proposed model of how increasing genomic vRNA capping negatively impacts viral infection.

We propose that, as diagrammed in Fig. 8, during wild-type infections, the translationally inactive ncgRNAs temper the molecular activities of the translationally active, capped genomic vRNA population, allowing the temporal progression of infection to lead to the assembly and release of viral particles. We postulate that the ncgRNAs, due to their lack of translational capacity, interact with a unique set of host factors relative to the capped translationally competent genomic RNAs. Collectively, these interactions lead to the development of a proassembly microenvironment by excluding host factors that either inhibit the assembly process or promote nucleocapsid disassembly. For instance, if the ncgRNAs foster a nontranslational environment through the interaction of host factors, such as those found within stress granules, the 60S ribosomal subunit, which is implicated in nucleocapsid disassembly, would be excluded from the local microenvironment, allowing assembly to occur unimpeded (40, 41). However, when the genomic RNA population was altered by increasing the efficiency of genomic RNA capping, such as was observed with the SINV D355A mutant, the increased and continuous translational activity of the genomic vRNA culminated in the formation of a protranslational vRNA “pool” that is refractory to encapsidation and particle assembly. Work examining such possibilities is ongoing in the laboratory of K. J. Sokoloski and will be reported in the future.

Conclusions. Collectively, these data affirm the existence and biological importance of the ncgRNAs during SINV infection. This assertion is directly supported by the capacity to modulate the capping activities of nsP1 protein via site-directed mutagenesis, resulting in increased production of XRN-1-resistant genomic vRNAs without increased overall genomic RNA numbers. Moreover, the preponderance of gene expression data indicating increased translation brought about by increasing the capping of the genomic vRNA supports the existence of the alphaviral ncgRNAs at a functional level. Finally, the molecular characterizations of SINV nsP1 mutant infections provide insight into the biological importance of the ncgRNAs with regard to the regulation of alphaviral infection at the molecular level.

MATERIALS AND METHODS

Tissue culture cells. BHK-21 cells (a gift from R. W. Hardy, Indiana University—Bloomington) were maintained in minimal essential media (MEM; Cellgro) containing 10% fetal bovine serum (FBS; Atlanta Biologicals), 1% antibiotic-antimycotic solution (Cellgro), 1% nonessential amino acids (Cellgro), and 1%

L-glutamine (Cellgro). Cells were cultured at 37°C and 5% CO₂ in a humidified incubator. Low-passage stocks were maintained via regular passaging using standard subculturing techniques.

Generation of SINV capping mutants. The SINV nsP1 mutants used in this study were generated either by site-directed mutagenesis or by Gibson assembly reactions. In particular, the SINV p389 Y286A and D355A mutants were generated via site-directed mutagenesis according to the instructions supplied with a Q5 site-directed mutagenesis kit (NEB). To this end, the parental wild-type strain consisting of the p389 SINV nsP3-GFP (nsP3-green fluorescent protein) reporter strain was PCR amplified with high-fidelity Q5 DNA polymerase using primer sets that incorporated the indicated alanine substitutions individually. Due to technical limitations that prevented the successful use of site-directed mutagenesis, the N376A mutant was generated by Gibson assembly via the use of a Gibson Ultra kit (SGI) through the use of restriction-digested p389 cDNA plasmid and a synthetic DNA fragment, according to the instructions of the manufacturers. SINV nanoluciferase reporter mutants, similarly to those previously described, were generated either by site-directed mutagenesis or by conventional restriction enzyme cloning schemes which swapped the GFP coding region of the existing p389 site mutants with a nanoluciferase coding region in a modular fashion (18).

In all cases, individual mutants were verified by whole-genome sequencing before subsequent analyses were performed. Full-genome sequences are available upon request. Highly similar phenotypes were observed for any given mutant in all virus backgrounds evaluated.

Production of SINV wild-type and mutant virus stocks. Wild type, Y286A, D355A, and N376A SINV p389 (a derivative of the Toto1101 strain containing GFP in frame with nsP3 [42]), as well as SINV pToto1101-nanoluc (a derivative of the Toto1101 strain containing nanoluciferase in frame with nsP3 [18]), were prepared by electroporation as previously described (43, 44). Briefly, 2.8×10^6 BHK-21 cells were electroporated with 10 µg of *in vitro*-transcribed RNA using a single pulse at 1.5 kV, 25 mA, and 200 Ω from a Gene Pulser Xcell system (Bio-Rad) as previously described (44). Cells were then incubated under normal incubation conditions until a cytopathic effect became apparent, at which point the supernatant was collected and clarified by centrifugation at $8,000 \times g$ for 10 min at 4°C. The clarified supernatant was then aliquoted into small-volume stocks, which were then stored at -80°C for later use.

Analysis of viral growth kinetics. To determine if mutation of the SINV nsp1 protein negatively affected infection, the viral growth kinetics of each of the individual strains described above were assayed in tissue culture models of infection. Essentially, BHK-21 cells were seeded in a 24-well plate and incubated under normal conditions. Once cell monolayers were 80% to 90% confluent, they were infected with either the wild-type parental virus or the individual capping mutant viruses at a multiplicity of infection (MOI) of 5 infectious units (IU) per cell. After a 1-h adsorption period, the inoculum was removed and the cells were washed twice with $1 \times$ phosphate-buffered saline (PBS) to remove unbound viral particles. Whole medium was added, and the cells were incubated at 37°C in a humidified incubator in the presence of 5% CO₂. At the indicated times post-infection, tissue culture supernatants were harvested (and the media replaced), and viral titer was determined via plaque assay.

Quantification of infectious virus by plaque assay. Standard virological plaque assays were used to determine the infectious titer of all viral samples produced during these studies. Briefly, BHK-21 cells were seeded in a 24-well plate and incubated under normal conditions. Once the cell monolayers were 80% to 90% confluent, they were inoculated with 10-fold serial dilutions of virus-containing samples. After a 1-h adsorption period, cells were overlaid with a solution of 0.5% Avicel (FMC Corporation) in $1 \times$ media for 28 to 30 h (45). The monolayers were fixed with formaldehyde solution (3.8% formaldehyde- $1 \times$ PBS) for a period of no less than 1 h. Plaques were visualized via staining with crystal violet after removal of the overlay and quantified by manual counting.

XRN1 protection assay/RppH assay. Viral genomic RNAs were extracted from purified viral particles harvested at 24 hpi. After extraction, the RNA samples were subjected to enzymatic degradation via use of the 5' to 3' exonuclease XRN-1, which is capable of degrading 5' monophosphate and RNAs *in vitro* but is unable to effectively degrade RNA substrates that are 5' capped (22, 23). Briefly, equivalent amounts of viral genomic RNAs were incubated in the presence of 0.25 units of XRN-1 (NEB) in a final volume of 20 µl for a period of 5 min at 37°C prior to being quenched via the addition of high-salt column buffer (25 mM Tris-HCl [pH 7.6]-400 mM NaCl-0.1% [wt/vol] sodium dodecyl sulfate [SDS]). After the termination of the reaction, the RNAs were purified via phenol-chloroform extraction and ethanol precipitation with linear acrylamide carrier. The resulting precipitate was resuspended and utilized as the substrate for the synthesis of cDNA via the use of ProtoScript II reverse transcriptase (NEB). The resulting cDNAs were quantified via quantitative PCR (qPCR) analysis of an amplicon located in the nsP1 region, as described below, to determine the sensitivity of a sample relative to wild-type viral genomic vRNAs (44, 46).

To confirm that the nature of the 5' end, in particular, the presence of a 5' cap structure, was responsible for the differences in XRN-1 sensitivity, the extracted RNAs were coincubated with XRN-1 in the presence of the decapping enzyme RppH (18, 24, 25). To this end, the reaction mixtures described above were supplemented with 1.25 units of RppH (NEB) and processed as described above.

Metabolic labeling of protein synthesis. To determine the rates of host and viral protein synthesis during infection, BHK-21 cells were seeded in a 12-well tissue culture dish and grown to 80% to 90% confluence prior to being infected with either the wild-type parental virus or one of the individual capping mutant viruses at an MOI of 10 IU/cell. After a 1-h adsorption period, fresh medium was added to each well, and the cells were incubated under the normal incubation conditions. Thirty minutes before the indicated times post-infection, the medium was removed and replaced with methionine- and cysteine-free Dulbecco's modified Eagle's medium (DMEM; Cellgro) to starve the cells of methionine. After a 30-min incubation period, the starvation medium was removed and replaced with methionine-

and cysteine-free DMEM supplemented with 50 μ M L-azidohomoalanine (L-AHA), a methionine analogue (47, 48). After 2 h, the labeling medium was removed, and the cells were washed with 1 \times PBS and then harvested with radioimmunoprecipitation assay (RIPA) buffer (50 mM Tris-HCl [pH 7.5]–150 mM NaCl–1% [vol/vol] Nonidet P-40 [NP-40]–0.5% [wt/vol] SDS–0.05% [wt/vol] sodium deoxycholate–1 mM EDTA). Cell lysates were labeled with DIBO-Alexa 648 (Invitrogen) at a final concentration of 5 μ M and incubated at room temperature in the dark for at least 1 h. The labeled lysates were then loaded onto a 12% SDS-PAGE gel, and the proteins were separated by electrophoresis. Fluorescence was then imaged using a Pharos FX Plus Molecular Imager (Bio-Rad), and the densitometry of individual protein species was used to quantify viral and host protein expression.

Western blot detection of SINV nsP2 protein expression. Whole-cell lysates were generated from BHK-21 cells infected with either the wild-type virus or the individual SINV nsP1 capping mutant viruses by resuspension in RIPA buffer at 12 and 16 hpi. Equivalent amounts of protein were loaded onto 10% acrylamide gels, and the individual protein species were resolved using standard SDS-PAGE practices. After sufficient resolution of the protein species, the proteins were transferred to polyvinylidene difluoride (PVDF) membranes, which were rinsed in methanol and thoroughly dried after transfer. After drying, the blots were probed with anti-SINV nsP2 polyclonal sera (a gift from R.W. Hardy at Indiana University—Bloomington) or with anti-actin (clone mAbGEa; Thermo Fisher Scientific) antibodies diluted in 1 \times PBS–1.0% (vol/vol) Tween (PBST) for a period of at least 1 h at 25°C with gentle rocking. The blots were washed three times with 1 \times PBST and were probed with fluorescent anti-rabbit (A32732; Thermo Fisher Scientific) and anti-mouse secondary (A32723; Thermo Fisher Scientific) antibodies. Protein detection was achieved using a Pharos FX Plus Molecular Imager (Bio-Rad), and the densitometry of individual protein species was used to quantify viral and protein expression.

qRT-PCR detection of SINV vRNAs. The quantitative detection of the SINV vRNAs was accomplished as previously described, with minor modifications (43). Briefly, to quantify the SINV genomic, subgenomic, and negative-sense vRNAs, BHK-21 cells were infected at an MOI of 5 IU/cell and cells were harvested at 2, 4, and 8 hpi via the addition of Ribozol (VWR). Total RNA was then isolated via extraction, and 1 μ g was reverse transcribed using Protoscript II reverse transcriptase (NEB) and a cocktail of specific RT primers based on the intended amplification targets. To detect the positive-sense RNA species, the RT primer cocktail consisted of nsP1, E1, and 18S reverse primers; to detect the minus-strand RNA species, the RT primer cocktail consisted of nsP1 forward and 18S reverse primers. The individual vRNA species were detected via the use of TaqMan probes and the following primer sets: for SINV nsP1, 5'-AAGGATCTCCGGACCGTA-3' forward (F) and 5'-AACATGAAGTGGTGTGTCGAAG-3' (reverse [R]); for SINV E1, 5'-TCAGATGCACCACTGGTCTCAACA-3' (F) and 5'-ATTGACCTTCGCGGTCGGATACAT-3' (R); for mammalian 18S, 5'-CGCGTCTCTTTTGTGGT-3' (F) and 5'-AGTCGGCATCGTTTATGGTC-3' (R). The sequences of the TaqMan detection probes used were as follows: SINV nsP1 probe, 5'-ACCATCGCTCTGTTTCAACGA-3'; SINV E1 probe, 5'-ACTTATTCAGCAGACTTCGGCGGG-3'; mammalian 18S probe, 5'-AAGACGGACCAGAGCGAAAGCAT-3'.

To quantify the total number of viral particles present in a sample, BHK-21 cells were infected at an MOI of 5 IU/cell and supernatant was collected at 24 hpi. As previously described, 5 μ l of supernatant was reverse transcribed (43). Reverse transcription and qPCR reactions were performed identically to those described above with the exception of the mammalian 18S primer and probes not being used. Absolute quantities of viral genomic RNAs were determined via the use of a standard curve of known concentrations.

Cell viability assay. To determine the effect of SINV infection on cell viability, BHK-21 cells were seeded in a 96-well plate and were infected with the wild-type parental virus or the individual capping mutant viruses at an MOI of 10 IU/cell. After a 1-h adsorption period, whole medium was added and the cells were incubated under normal incubation conditions for the indicated times. Afterward, the cells were washed with 1 \times PBS and a solution of 1/6 CellTiter 96 AQ_{ueous} One Solution reagent (Promega)–1 \times PBS was added to each well. The cells were then allowed to incubate at 37°C and 5% CO₂ for 2 h. Absorbance at 490 nm was then recorded using a Synergy H1 microplate reader (BioTek).

Quantification of viral gene expression via nanoluciferase assays. To quantify genomic translation during infection, BHK-21 cells were infected at an MOI of 5 IU/cell with the wild-type parental virus or the individual capping mutants containing the nanoluciferase gene within the nsP3 protein (18). After a 1-h period of adsorption on ice, the inoculum was removed and the medium was replaced with prewarmed whole medium. The infected cells were incubated under normal conditions, and at the indicated times post-infection, the medium was removed and the tissue culture cells were washed with 1 \times PBS. The cells were then harvested into a crude lysate by the addition of 1 \times PBS supplemented with 0.5% (vol/vol) Triton X-100. The lysate was transferred to a microcentrifuge tube and frozen until the completion of the experimental time course. The samples were thawed and clarified by centrifugation at 16,000 \times g for 5 min, and equal cell volumes of the nanoluciferase samples were processed using a Nano-Glo nanoluciferase assay system (Promega) according to the manufacturer's instructions. Luminescence was then recorded using a Synergy H1 microplate reader (BioTek).

Statistical analysis. The quantitative data reported in this study represent means of data from a minimum of three independent biological replicates, unless specifically noted otherwise. The growth curve data presented in Fig. 2 were statistically assessed using an area-under-the-curve approach to determine differences in viral growth kinetics throughout the course of the assay. The statistical analysis of comparative samples was performed as previously described (43), using variable bootstrapping where appropriate. The error bars indicate standard deviations of the means. The *P* values associated with individual quantitative data sets were determined using Student's *t* test for the corresponding quantitative data.

ACKNOWLEDGMENTS

We thank the members of the laboratories of K. J. Sokoloski, D. Chung, and I. S. Lukashevich for their input during the development of the project and the preparation/editing of the manuscript. In addition, we thank Susana Lopez for the opportunity to host Joaquín Moreno-Contreras during the course of this work.

This work was funded by a grant from the National Institute of Allergy and Infectious Diseases, specifically, grant R21 AI121450 (to K.J.S. and Richard W. Hardy), and by a pilot grant supported by a COBRE program from the National Institute of General Medical Sciences, specifically grant P20 GM125504 (to K.J.S. and R. Lamont). Additional support for this research consisted of a generous startup package from the University of Louisville (to K.J.S.), support from the Integrated Programs in Biomedical Sciences (IPIBS; to A.T.L.), and funds from the Department of Microbiology and Immunology of the School of Medicine at the University of Louisville (to K.J.S.). A.T.L. was supported by an NIH-NIAID funded predoctoral fellowship, T32 AI132146.

The research efforts of J.M.-C. were supported by funds received from the Scientific Short Visit program sponsored by CONACyT and PAEP/UNAM.

REFERENCES

- Calisher CH. 1994. Medically important arboviruses of the United States and Canada. *Clin Microbiol Rev* 7:89–116. <https://doi.org/10.1128/CMR.7.1.89>.
- de la Monte S, Castro F, Bonilla NJ, Gaskin de Urdaneta A, Hutchins GM. 1985. The systemic pathology of Venezuelan equine encephalitis virus infection in humans. *Am J Trop Med Hyg* 34:194–202. <https://doi.org/10.4269/ajtmh.1985.34.194>.
- Adouchief S, Smura T, Sane J, Vapalahti O, Kurkela S. 2016. Sindbis virus as a human pathogen-epidemiology, clinical picture and pathogenesis. *Rev Med Virol* 26:221–241. <https://doi.org/10.1002/rmv.1876>.
- Kurkela S, Helve T, Vaheeri A, Vapalahti O. 2008. Arthritis and arthralgia three years after Sindbis virus infection: clinical follow-up of a cohort of 49 patients. *Scand J Infect Dis* 40:167–173. <https://doi.org/10.1080/00365540701586996>.
- Kurkela S, Manni T, Myllynen J, Vaheeri A, Vapalahti O. 2005. Clinical and laboratory manifestations of Sindbis virus infection: prospective study, Finland, 2002–2003. *J Infect Dis* 191:1820–1829. <https://doi.org/10.1086/430007>.
- Harley D, Sleight A, Ritchie S. 2001. Ross River virus transmission, infection, and disease: a cross-disciplinary review. *Clin Microbiol Rev* 14:909–932. <https://doi.org/10.1128/CMR.14.4.909-932.2001>.
- Rulli NE, Suhrbier A, Hueston L, Heise MT, Tupanceska D, Zaid A, Wilmes A, Gilmore K, Lidbury BA, Mahalingam S. 2005. Ross River virus: molecular and cellular aspects of disease pathogenesis. *Pharmacol Ther* 107:329–342. <https://doi.org/10.1016/j.pharmthera.2005.03.006>.
- Pettersson RF. 1981. 5'-Terminal nucleotide sequence of Semliki forest virus 18S defective interfering RNA is heterogeneous and different from the genomic 42S RNA. *Proc Natl Acad Sci U S A* 78:115–119. <https://doi.org/10.1073/pnas.78.1.115>.
- Pettersson RF, Soderlund H, Kaariainen L. 1980. The nucleotide sequences of the 5'-terminal T1 oligonucleotides of Semliki-Forest-virus 42-S and 26-S RNAs are different. *Eur J Biochem* 105:435–443. <https://doi.org/10.1111/j.1432-1033.1980.tb04518.x>.
- Cancedda R, Shatkin AJ. 1979. Ribosome-protected fragments from Sindbis 42-S and 26-S RNAs. *Eur J Biochem* 94:41–50. <https://doi.org/10.1111/j.1432-1033.1979.tb12869.x>.
- Mi S, Stollar V. 1991. Expression of Sindbis virus nsP1 and methyltransferase activity in *Escherichia coli*. *Virology* 184:423–427. [https://doi.org/10.1016/0042-6822\(91\)90862-6](https://doi.org/10.1016/0042-6822(91)90862-6).
- Ahola T, Kaariainen L. 1995. Reaction in alphavirus mRNA capping: formation of a covalent complex of nonstructural protein nsP1 with 7-methyl-GMP. *Proc Natl Acad Sci U S A* 92:507–511. <https://doi.org/10.1073/pnas.92.2.507>.
- Vasiljeva L, Merits A, Auvinen P, Kaariainen L. 2000. Identification of a novel function of the alphavirus capping apparatus. RNA 5'-triphosphatase activity of Nsp2. *J Biol Chem* 275:17281–17287. <https://doi.org/10.1074/jbc.M910340199>.
- Li C, Guillen J, Rabah N, Blanjoie A, Debart F, Vasseur JJ, Canard B, Decroly E, Coutard B. 2015. mRNA capping by Venezuelan equine encephalitis virus nsP1: functional characterization and implications for antiviral research. *J Virol* 89:8292–8303. <https://doi.org/10.1128/JVI.00599-15>.
- Wang HL, O'Rear J, Stollar V. 1996. Mutagenesis of the Sindbis virus nsP1 protein: effects on methyltransferase activity and viral infectivity. *Virology* 217:527–531. <https://doi.org/10.1006/viro.1996.0147>.
- Ahola T, Laakkonen P, Vihinen H, Kaariainen L. 1997. Critical residues of Semliki Forest virus RNA capping enzyme involved in methyltransferase and guanylyltransferase-like activities. *J Virol* 71:392–397.
- Hefti E, Bishop DH, Dubin DT, Stollar V. 1975. 5' nucleotide sequence of Sindbis viral RNA. *J Virol* 17:149–159.
- Sokoloski KJ, Haist KC, Morrison TE, Mukhopadhyay S, Hardy RW. 2015. Noncapped alphavirus genomic RNAs and their role during infection. *J Virol* 89:6080–6092. <https://doi.org/10.1128/JVI.00553-15>.
- Stoermer Burrack KA, Hawman DW, Jupille HJ, Oko L, Minor M, Shives KD, Gunn BM, Long KM, Morrison TE. 2014. Attenuating mutations in nsP1 reveal tissue-specific mechanisms for control of Ross River virus infection. *J Virol* 88:3719–3732. <https://doi.org/10.1128/JVI.02609-13>.
- Yang J, Yan R, Roy A, Xu D, Poisson J, Zhang Y. 2015. The I-TASSER Suite: protein structure and function prediction. *Nat Methods* 12:7–8. <https://doi.org/10.1038/nmeth.3213>.
- Ahola T, Karlin DG. 2015. Sequence analysis reveals a conserved extension in the capping enzyme of the alphavirus supergroup, and a homologous domain in nodaviruses. *Biol Direct* 10:16. <https://doi.org/10.1186/s13062-015-0050-0>.
- Stevens A, Poole TL. 1995. 5'-Exonuclease-2 of *Saccharomyces cerevisiae*. Purification and features of ribonuclease activity with comparison to 5'-exonuclease-1. *J Biol Chem* 270:16063–16069. <https://doi.org/10.1074/jbc.270.27.16063>.
- Jinek M, Coyle SM, Doudna JA. 2011. Coupled 5' nucleotide recognition and processivity in Xrn1-mediated mRNA decay. *Mol Cell* 41:600–608. <https://doi.org/10.1016/j.molcel.2011.02.004>.
- Song MG, Bail S, Kiledjian M. 2013. Multiple Nudix family proteins possess mRNA decapping activity. *RNA* 19:390–399. <https://doi.org/10.1261/ma.037309.112>.
- Hetzl J, Duttke SH, Benner C, Chory J. 2016. Nascent RNA sequencing reveals distinct features in plant transcription. *Proc Natl Acad Sci U S A* 113:12316–12321. <https://doi.org/10.1073/pnas.1603217113>.
- Shatkin AJ. 1976. Capping of eucaryotic mRNAs. *Cell* 9:645–653. [https://doi.org/10.1016/0092-8674\(76\)90128-8](https://doi.org/10.1016/0092-8674(76)90128-8).
- Banerjee AK. 1980. 5'-Terminal cap structure in eucaryotic messenger ribonucleic acids. *Microbiol Rev* 44:175–205.
- Sonenberg N, Gingras AC. 1998. The mRNA 5' cap-binding protein eIF4E and control of cell growth. *Curr Opin Cell Biol* 10:268–275. [https://doi.org/10.1016/S0955-0674\(98\)80150-6](https://doi.org/10.1016/S0955-0674(98)80150-6).
- Fros JJ, Pijlman GP. 2016. Alphavirus infection: host cell shut-off and

- inhibition of antiviral responses. *Viruses* <https://doi.org/10.3390/v8060166>.
30. Castello A, Sanz MA, Molina S, Carrasco L. 2006. Translation of Sindbis virus 26S mRNA does not require intact eukariotic initiation factor 4G. *J Mol Biol* 355:942–956. <https://doi.org/10.1016/j.jmb.2005.11.024>.
 31. Kim DY, Firth AE, Atasheva S, Frolova EI, Frolov I. 2011. Conservation of a packaging signal and the viral genome RNA packaging mechanism in alphavirus evolution. *J Virol* 85:8022–8036. <https://doi.org/10.1128/JVI.00644-11>.
 32. Rupp JC, Jundt N, Hardy RW. 2011. Requirement for the amino-terminal domain of Sindbis virus nsP4 during virus infection. *J Virol* 85:3449–3460. <https://doi.org/10.1128/JVI.02058-10>.
 33. Fata CL, Sawicki SG, Sawicki DL. 2002. Modification of Asn374 of nsP1 suppresses a Sindbis virus nsP4 minus-strand polymerase mutant. *J Virol* 76:8641–8649. <https://doi.org/10.1128/JVI.76.17.8641-8649.2002>.
 34. Shirako Y, Strauss EG, Strauss JH. 2000. Suppressor mutations that allow Sindbis virus RNA polymerase to function with nonaromatic amino acids at the N-terminus: evidence for interaction between nsP1 and nsP4 in minus-strand RNA synthesis. *Virology* 276:148–160. <https://doi.org/10.1006/viro.2000.0544>.
 35. Kumar S, Kumar A, Mamidi P, Tiwari A, Kumar S, Mayavannan A, Mudulli S, Singh AK, Subudhi BB, Chattopadhyay S. 2018. Chikungunya virus nsP1 interacts directly with nsP2 and modulates its ATPase activity. *Sci Rep* 8:1045. <https://doi.org/10.1038/s41598-018-19295-0>.
 36. Jupille HJ, Oko L, Stoermer KA, Heise MT, Mahalingam S, Gunn BM, Morrison TE. 2011. Mutations in nsP1 and PE2 are critical determinants of Ross River virus-induced musculoskeletal inflammatory disease in a mouse model. *Virology* 410:216–227. <https://doi.org/10.1016/j.virol.2010.11.012>.
 37. Kallio K, Hellstrom K, Jokitalo E, Ahola T. 2016. RNA replication and membrane modification require the same functions of alphavirus non-structural proteins. *J Virol* 90:1687–1692. <https://doi.org/10.1128/JVI.02484-15>.
 38. Gonzalez-Almela E, Sanz MA, Garcia-Moreno M, Northcote P, Pelletier J, Carrasco L. 2015. Differential action of pateamine A on translation of genomic and subgenomic mRNAs from Sindbis virus. *Virology* 484:41–50. <https://doi.org/10.1016/j.virol.2015.05.002>.
 39. Patel RK, Burnham AJ, Gebhart NN, Sokoloski KJ, Hardy RW. 2013. Role for subgenomic mRNA in host translation inhibition during Sindbis virus infection of mammalian cells. *Virology* 441:171–181. <https://doi.org/10.1016/j.virol.2013.03.022>.
 40. Singh I, Helenius A. 1992. Role of ribosomes in Semliki Forest virus nucleocapsid uncoating. *J Virol* 66:7049–7058.
 41. Wengler G, Wengler G. 1984. Identification of a transfer of viral core protein to cellular ribosomes during the early stages of alphavirus infection. *Virology* 134:435–442. [https://doi.org/10.1016/0042-6822\(84\)90310-6](https://doi.org/10.1016/0042-6822(84)90310-6).
 42. Frolova E, Gorchakov R, Garmashova N, Atasheva S, Vergara LA, Frolov I. 2006. Formation of nsP3-specific protein complexes during Sindbis virus replication. *J Virol* 80:4122–4134. <https://doi.org/10.1128/JVI.80.8.4122-4134.2006>.
 43. Sokoloski KJ, Hayes CA, Dunn MP, Balke JL, Hardy RW, Mukhopadhyay S. 2012. Sindbis virus infectivity improves during the course of infection in both mammalian and mosquito cells. *Virus Res* 167:26–33. <https://doi.org/10.1016/j.virusres.2012.03.015>.
 44. LaPointe AT, Gebhart NN, Meller ME, Hardy RW, Sokoloski KJ. 10 January 2018. The identification and characterization of Sindbis virus RNA:host protein interactions. *J Virol* <https://doi.org/10.1128/JVI.02171-17>.
 45. Baer A, Kehn-Hall K. 4 November 2014. Viral concentration determination through plaque assays: using traditional and novel overlay systems. *J Vis Exp* <https://doi.org/10.3791/52065>.
 46. Garneau NL, Sokoloski KJ, Opyrchal M, Neff CP, Wilusz CJ, Wilusz J. 2008. The 3' untranslated region of Sindbis virus represses deadenylation of viral transcripts in mosquito and mammalian cells. *J Virol* 82:880–892. <https://doi.org/10.1128/JVI.01205-07>.
 47. Best MD. 2009. Click chemistry and bioorthogonal reactions: unprecedented selectivity in the labeling of biological molecules. *Biochemistry* 48:6571–6584. <https://doi.org/10.1021/bi9007726>.
 48. Sokoloski KJ, Nease LM, May NA, Gebhart NN, Jones CE, Morrison TE, Hardy RW. 2017. Identification of interactions between Sindbis virus capsid protein and cytoplasmic vRNA as novel virulence determinants. *PLoS Pathog* 13:e1006473. <https://doi.org/10.1371/journal.ppat.1006473>.